J. Chem. Sci. Vol. 127, No. 7, July 2015, pp. 1155–1166.
DOI 10.1007/s12039-015-0876-0

Hydroxy, carboxylic and amino acid functionalized superparamagnetic iron oxide nanoparticles: Synthesis, characterization and *in vitro* anti-cancer studies

DILAVEEZ REHANA[a,b], AZEES KHAN HALEEL[a] and AZIZ KALILUR RAHIMAN[a,*]

[a]Post-Graduate and Research Department of Chemistry, The New College (Autonomous), Chennai 600 014, India

[b]Justice Basheer Ahamed Sayeed College for Women (Autonomous), Chennai 600 018, India

e-mail: akrahmanjkr@gmail.com

MS received 5 September 2014; revised 28 February 2015; accepted 4 March 2015

Abstract. Superparamagnetic iron oxide nanoparticles were synthesized by simple co-precipitation method and modified with different coating agents such as ascorbic acid, hexanoic acid, salicylic acid, L-arginine and L-cysteine. The synthesized nanoparticles were characterized by various techniques such as FT IR, XRD, VSM, SEM, TEM and thermal analysis. Both bare and coated magnetites were of cubic spinel structure and spherical in shape. All the magnetite nanoparticles showed superparamagnetic behaviour with high saturated magnetization. *In vitro* cytotoxicity test of bare and coated nanoparticles was performed using adenocarcinoma cells, A549. Cell viability of bare and L-arginine coated magnetite nanoparticles showed IC_{50} value of 31.2 μg/mL proving the compatibility of nanocarriers when compared to others. Hence, L-arginine coated nanoparticles were used for loading the drug paclitaxel and the observed IC_{50} value (7.8 μg/mL) shows its potent anti-proliferative effect against A549 lung cancer cell lines. Thus, it can be speculated that the drug paclitaxel loaded L-arginine coated nanoparticles could be used as an effective drug carrier for the destruction of cancer cells.

Keywords. Magnetite nanoparticles; acid-coated magnetite nanoparticles; cytotoxicity; DNA fragmentation.

1. Introduction

In recent years, nanoparticles have attracted considerable attention because of their potential medicinal applications such as cellular therapy involving cell labelling and targeting as a tool for cell biology research to separate and purify cell population, tissue repair, targeted drug delivery, magnetic resonance imaging and hyperthermia for cancer treatment.[1] Most of these applications require the nanoparticles to be uniform in size and shape and well-dispersed in solvents, which are generally controlled by synthesis method.[2] The magnetic nanoparticles have gained increasing attention for use in biomedical applications. Among these, iron oxide is one of the most important transition metal oxides. Sixteen pure phases of iron oxide i.e.,oxide, hydroxide or oxy-hydroxides are known to date; these are $Fe(OH)_3$, $Fe(OH)_2$, Fe_5HO_8-$4H_2O$, Fe_3O_4 FeO, five polymorphs of FeOOH, and four Fe_2O_3. Magnetite (Fe_3O_4) is a black ferromagnetic mineral containing both Fe(II) and Fe(III).[3] It has cubic inverse spinel structure with fcc close-packed oxygen and iron ions occupying interstitial tetrahedral and octahedral sites.[4] In the nano-realm, Fe_3O_4 particles exhibit superparamagnetic behaviour at room temperature, i.e., they magnetize strongly under the applied magnetic field but do not retain this property once the field is removed. This nature makes them suitable for biomedical applications.[5] Superparamagnetic iron oxide has been recognized as a promising tool for site specific delivery of drugs and diagnostic agent.[6] To date, these nanoparticles are known to be low in toxicity and biocompatibile. These features make it an ideal material for *in vitro* studies.[7]

The surface functionalization of magnetite nanoparticles with a biological or chemical agent which binds to a specific target has been of great interest in recent years.[8] The functionalization of nanoparticles improve their biocompatibility, avoid aggregation among the particles by magnetic forces and provides the specific functionilization to cancer cells.[9] To impart functionality and conjugate with biologically active agents, iron oxide nanoparticles are usually coated with functional groups on their surface, such as phosphate, sulphate, carboxylate, etc. Of these functional groups, carboxylate is the strongest binder. The carboxyl/hydroxyl group gets chemisorbed to the nanoparticles forming a carboxylate group with Fe-OH molecules leaving

*For correspondence

any other group present for various purposes.[10] Several anti-cancer drugs including doxorubicin, 5-fluorouracil, dexamethasone and paclitaxel have been successfully formulated using nanomaterials, which can either be integrated in the matrix of particles or attached to the particle surface.[11] Drug delivery using superparamagnetic nanoparticles can be manipulated by external magnetic field.[12] The drug loaded magnetic nanoparticles have been investigated for various biomedical application such as DNA separation, drug delivery, magnetic resonance imaging, and hyperthermia.[13]

This paper describes the synthesis of non-toxic and biocompatible Fe_3O_4 nanoparticles functionalized with different acids such as ascorbic acid, hexanoic acid, salicylic acid, L-arginine and L-cysteine by co-precipitation method, which allows targeted drug delivery to the cancer cell lines thereby reducing the systemic toxicity of the anti-cancer drug. The effect of the crystal structure, morphology and magnetic properties of bare and modified Fe_3O_4 were investigated. Further, all the acid coated nanoparticles and paclitaxel drug loaded L-arginine coated nanoparticles were evaluated for their *in vitro* cytotoxicity on adenocarcinoma cells A549 using MTT assay. It was found that positively charged L-arginine coated nanoparticles demonstrated a significant amount of cytotoxicity with IC_{50} value of 31.2 μg/mL when compared to the negatively charged carboxylic and hydroxy acids (ascorbic acid, salicylic acid or hexanoic acid) coated nanoparticles. The nanoparticles functionalized with L-arginine exhibit highest cytotoxic effect, and hence subjected to DNA fragmentation by agarose gel electrophoresis.

2. Experimental

2.1 *Materials*

Ferrous chloride tetrahydrate ($FeCl_2.4H_2O$) and ferric chloride anhydrous ($FeCl_3$) were used as the precursor and purchased from Sigma-Aldrich. Ascorbic acid, hexanoic acid, salicylic acid, L-arginine and L-cysteine were used as coating agent and purchased from Merck. All the materials were analytical grade and used without further purification. Solvents were dried and purified before being used according to standard procedure.

2.2 *Synthesis of magnetic nanoparticles*

Synthesis of magnetite (Fe_3O_4) nanoparticles was carried out by chemical co-precipitation method in a nitrogen atmosphere as per the reported procedure with little modification. [2] $FeCl_2.4H_2O$ and $FeCl_3$ with the molar ratio of ferric to ferrous ion 0.01:0.007 were dissolved in 100 mL deionised water and 25 wt% NH_4OH was added slowly to achieve complete precipitation of iron oxide. Coating agent (Ascorbic acid, hexanoic acid, salicylic acid, L-arginine or L-cysteine) was added at a concentration of 0.07% to the above solution with vigorous stirring. On addition of the hydroxy and carboxylic acid, the solution became yellow in colour which then turned to black on vigorous stirring. When the amino acids were added, the solution became dark blue which then turned to black on vigorous stirring. The modified magnetite nanoparticles were filtered, thoroughly washed with deionized water to remove chloride ions, then washed several times with ethanol to remove excess coating agent, and finally dried in vacuum at 80°C for 24 h. The bare magnetite nanoparticles were also prepared by adopting same procedure without adding coating agent. The samples are denoted as S–S7; S-Bare magnetite nanoparticles, S1–Ascorbic acid coated magnetite nanoparticles, S2–Hexanoic acid coated magnetite nanoparticles, S3–Salicylic acid coated magnetite nanoparticles, S4–L-arginine coated magnetite nanoparticles, S5–L-cysteine coated magnetite nanoparticles, S6–Drug paclitaxel, S7–Paclitaxel loaded L-arginine coated magnetite nanoparticles.

2.3 *Characterization*

FT IR measurements were carried out on Shimadzu IR460 spectrophotometer in the range 4000–400 cm^{-1} using KBr pellets. The crystalline structure of the nanoparticles was determined using X-ray diffraction (XRD) on a Siefert Analyze diffractometer operated at 40 Kv and 35 mA with Cu Kα radiation ($\lambda = 0.15406$ Å). The hydrodynamic size and the zeta potential distribution of nanoparticles were measured on Malvern Zetasizer Ver 6.20 (Malvern instruments, UK). Magnetization (M_S) values of dried magnetite nanoparticles were evaluated at room temperature by Lakeshore vibrating sample magnetometer model 7410. The morphology was studied by a Field Emission Scanning Electron Microscope (FESEM) at 10 to 30 kV (Hitachi SU6600). The particle size and size distribution were calculated from TEM image of nanoparticles on Philips Technai at 180 kV. The thermal stability was determined by thermogravimetric analysis (Netzsch STA 409 TGA/DSC). The thermogram was recorded for 5 mg of powder sample at a heating rate of 10°C per min in the temperature of 30–800°C under nitrogen atmosphere.

2.4 *Cytotoxitcity*

Human lung adenocarcinoma (A549) cancer cell lines were obtained from National Centre for Cell Sciences

(NCCS), Pune, India. The cells were maintained in Minimal Essential Media supplemented with 10% Fetal Bovine Serum (FBS), penicillin (100 μg/mL) and streptomycin (100 μg/mL) in a humidified atmosphere of 5% CO_2 at 37°C.

The anti-cancer activity of bare and coated magnetite nanoparticles was determined by MTT (3-(4,5-dimethyl-2-thiazolyl)-2,5-diphenyltetrazolium bromide) assay. The A549 cells (1×10^5/well) were plated in 0.2 mL of medium/well in 96-well plate and treated with bare and coated magnetite nanoparticles suspension at different concentrations (10–1000 μg/mL) and incubated for 72 h at 37°C in a 5% CO_2 incubator for better cell attachment. Thereafter, the wells were washed with warm phosphate buffered saline solution and incubated again for 4 h with DMEM containing 25 μL of 5.5 mg/mL MTT solution. After discarding the culture medium, 1 mL of DMSO was added to dissolve the precipitate, and the resultant solution was measured at 540 nm. The inhibitory concentration value (IC_{50}) was determined from the absorbance *versus* the concentration curves. The experiment was carried out in triplicate and the values are expressed as mean ±SD.

2.5 *DNA Fragmentation*

Inter-nucleosomal cleavage of DNA was analysed as described previously.[14] The cells were incubated with L-arginine coated nanoparticles for 48 h followed by cell detachment using trypsin-EDTA and washed with phosphate buffered saline solution. The cell pellets were incubated with 200 μL at 5% CO_2 with protein precipitation solution. After centrifugation, the supernatant containing the DNA was separated and mixed with 600 μL isopropanol followed by centrifugation and mixing the pellets with DNA sample solution at 65°C for 1 h. DNA bands were separated using 2% agarose gel electrophoresis containing ethidium bromide and visualized using UV trans illuminator. The untreated cells were used as a negative control.

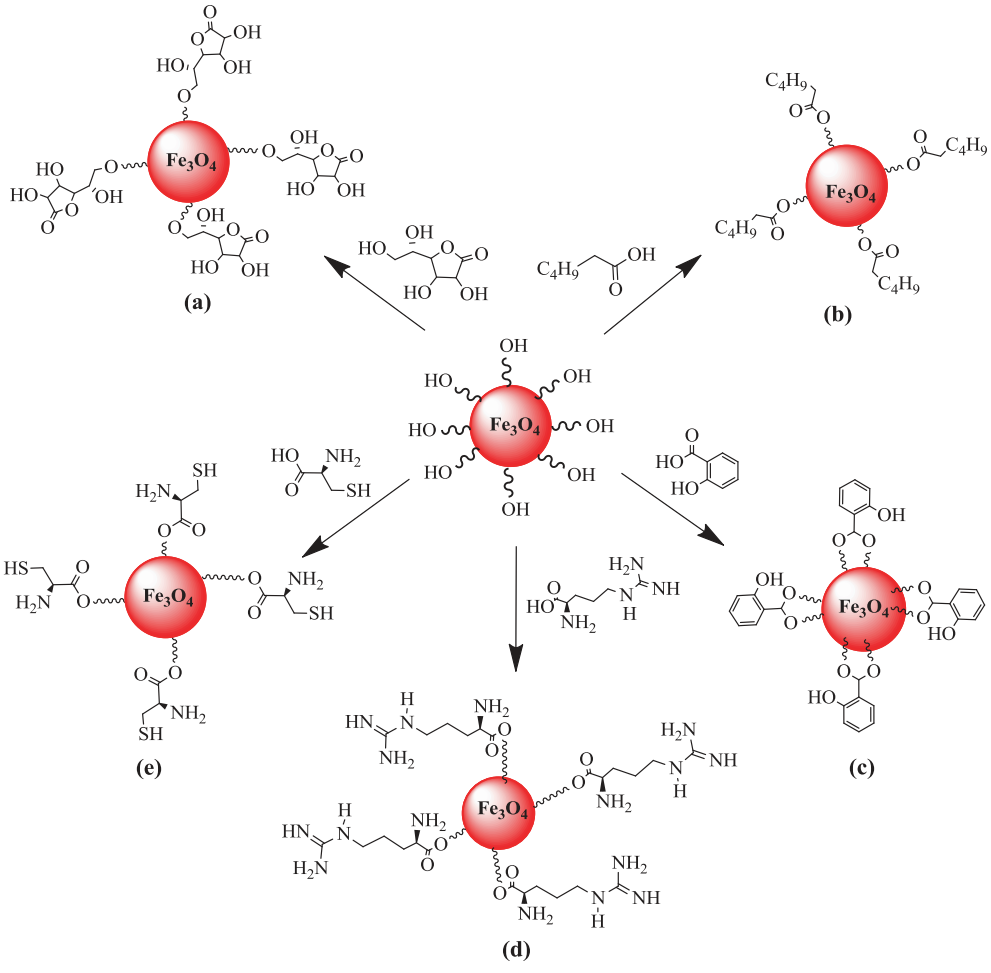

Figure 1. Schematic representation of esterification of iron oxide nanoparticles with different coating agents (**a**) Ascorbic acid; (**b**) Hexanoic acid; (**c**) Salicylic acid; (**d**) L-Arginine; and (**e**) L-Cysteine.

3. Results and Discussion

Iron oxide nanoparticles were synthesized by co-precipitation method using aqueous Fe^{2+}/Fe^{3+} by the addition of a base under inert atmosphere at elevated temperature. A black coloured precipitate was obtained which was washed and dried. There was no colour change between bare and coated iron oxide nanoparticles. Flow of nitrogen not only protects oxidation but also reduces the size of the particle. Ammonium hydroxide plays a key role in the formation of Fe_3O_4. It acts as a pH buffer and reacts with water to give constant supply of OH^- ions.[15] The reaction involved in this process is expressed as follows.[16]

$$Fe^{2+} + 2Fe^{3+} + 8OH^- \rightarrow Fe_3O_4 \text{ (black colloidal particles)} + 4H_2O$$

$$Fe_3O_4 + 0.25O_2 + 4.5H_2O \rightarrow 3Fe(OH)_3$$

During the coating process, acid was chemically adsorbed on to the magnetite nanoparticles which then undergo esterification between the hydroxyl, amino and carboxyl groups of the different coating agents. Schematic representations of functionalized nanoparticles are shown in figure 1. It is reported that magnetic nanoparticles prepared by co-precipitation method have a number of hydroxyl groups on the surface.[17] Hence, the interaction between the coating material containing carboxyl or hydroxyl groups which acts as a hydrogen bond acceptor or donor with the magnetite nanoparticles takes place through hydrogen bond.[18]

3.1 *FT IR analysis*

FT IR spectra of bare and coated magnetite nanoparticles are shown in figure 2. The characteristic band at 590 cm^{-1} indicative of Fe-O present in Fe_3O_4.[16] This band is shifted to 574–584 cm^{-1} for acid coated materials indicating successful functionalization on the surface of the magnetite nanoparticles. These bands are attributed to the intrinsic vibration of iron ion in tetrahedral and octahedral sites of spinel structure, respectively. It was also reported that the magnetite nanoparticles take up hydroxy groups on the surface upon contact with aqueous phase through adsorption of OH^- ion on Fe and H^+ on O.[19] The band at 1633 cm^{-1} is assigned to the OH stretching vibration of Fe_3O_4. The appearance of band at 1600–1630 cm^{-1} corresponds to stretching vibration of C=O for the coated nanoparticles. The band at 2840–2855 cm^{-1} and 2920–2955 cm^{-1} are assigned to CH_2 symmetric and asymmetric stretching of all the functionalized nanoparticles except salicylic acid coated nanoparticles.[20] The band at 1400–1431 cm^{-1} and 1530–1552 cm^{-1} corresponds to the asymmetric and symmetric stretching vibrations of carboxyl group (COO^-) of coating agents except ascorbic acid. Here, two binding modes have been suggested. In one mode, carboxylate is connected to the surface through one oxygen atom giving rise to symmetric and asymmetric vibrations, while in the other mode it is bound symmetrically to the surface giving rise to only stretching vibrations. The combination of molecules bonded symmetrically and molecules bonded at an angle by the carboxylic acid on the surface of magnetite nanoparticles is thus explained.[21] However, the ascorbic acid coated material showed two strong bands at 1024 and 1091 cm^{-1} corresponding to the symmetric stretching mode of C-O-C vibration. The L-arginine coated nanoparticles exhibit a band at 1637 cm^{-1} corresponding to NH bending and a broad band could be visualized in the range 3377–3398 cm^{-1} indicative of the presence of NH_2 and OH group on the surface of the nanoparticles. The observed sharp band at 2360 cm^{-1} for L-cysteine functionalized magnetite nanoparticles is due to the presence of SH onto the surface of nanoparticles.[22]

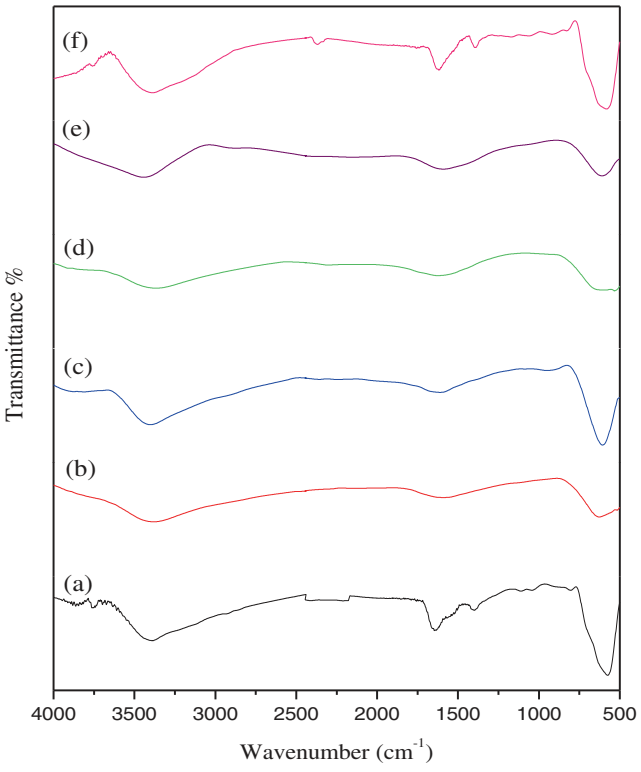

Figure 2. FT-IR spectra of (**a**) Fe_3O_4 nanoparticles; and nanoparticles coated with (**b**) Ascorbic acid; (**c**) Hexanoic acid; (**d**) Salicylic acid; (**e**) L-Arginine; (**f**) L-Cysteine.

3.2 *XRD analysis*

Powder XRD analysis revealed information about crystallographic structure, chemical composition and physical properties of the synthesized nano materials (figure 3). XRD pattern of magnetite exhibit the characteristic 110, 220, 311, 400, 422, 511 and 540 peaks of Fe_3O_4 crystal with a cubic spinel structure at $\sim 2\theta$ of 30°, 35°, 43°, 53°, 57° and 74°, respectively.[2] Crystallinity and morphology of bare and coated iron oxide nanoparticles have been affected by different groups such as phosphates, carboxyl etc have also been reported.[23] The most intense peak (311) appeared for both bare and acid functionalized Fe_3O_4 corresponds to reflection of Fe_3O_4 related to the mean size of the crystal according to Scherrer equation.[16] The XRD pattern of the coated Fe_3O_4 materials indicate that the coating agent does not significantly affect the crystal structure of the magnetite nanoparticles. The Fe_3O_4 peak (110) weakened in the coated material which is probably caused by the coating of different acids on the surface of magnetite nanoparticles.

However, XRD pattern of the coated magnetite nanoparticles depicted same peaks but the intensity varied due to the organic material present in it proving that coating agent helps in reducing the crystalline size without affecting the crystal structure. The peaks such as 311, 400 and 422, of the coated Fe_3O_4 nanoparticles were selected for good fit correlation, half maximum width, average crystalline size and size distribution using Scherrer equation which resulted in error due to low fit correlation and poor crystallization.[24]

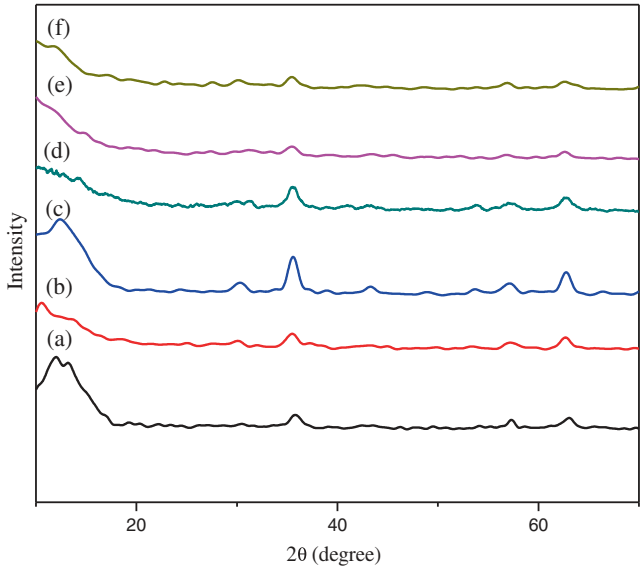

Figure 3. XRD pattern of (**a**) Fe_3O_4 nanoparticles; and nanoparticles coated with (**b**) Ascorbic acid; (**c**) Hexanoic acid; (**d**) Salicylic acid; (**e**) L-Arginine; (f) L-Cysteine.

3.3 *Zeta potential and particle size measurements*

The stability of the nanoparticles were characterized by zeta potential value (figure 4). A lower zeta potential value means less charge and may be related to shorter adsorption time.[10] L-Arginine functionalized nanoparticles do not exhibit good stabilization due to the fact that they do not possess electrostatic stabilization but have steric stabilization and hence have less zeta potential value of 3.8 mV. Hexanoic acid coated iron oxide nanoparticles have zeta potential value of 21.2 mV and are also unstable; this may be due to the agglomeration of the nanoparticles. L-Arginine due to steric stabilization property and also the positive surface charge on the amino group plays a critical role in non-specifically sticking to the cells, entering into it and destroying it.

The average particle size measured by dynamic light scattering (DLS) analysis for L-arginine and hexanoic acid coated iron oxide nanoparticles are 30 nm and 195 nm, respectively (figure 5). Particles were seen to aggregate due to strong dipole interaction, coating with pendant functional groups imparted stability by electrostatic repulsion. In the case of L-arginine coated

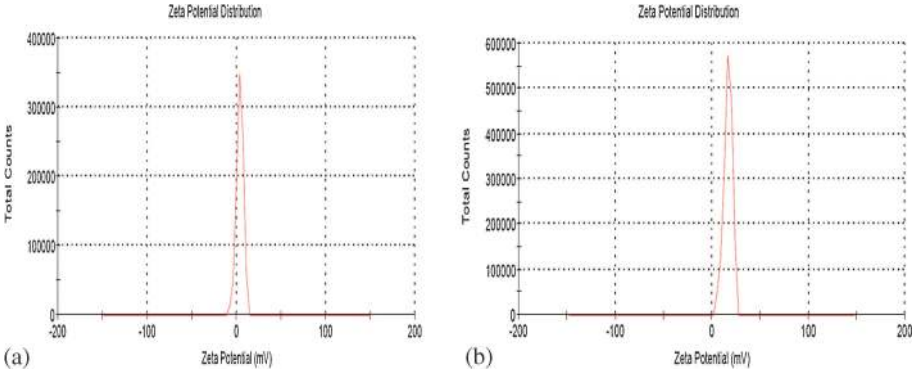

Figure 4. The zeta potential measurement of (**a**) L-Arginine coated Fe_3O_4 nanoparticles; (**b**) Hexanoic acid coated Fe_3O_4 nanoparticles.

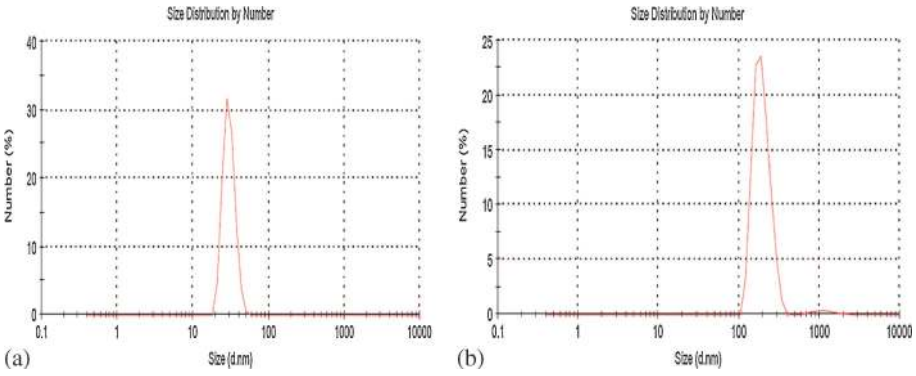

Figure 5. The particle size distribution of (**a**) L-Arginine coated Fe_3O_4 nanoparticles; and (**b**) Hexanoic acid coated Fe_3O_4 nanoparticles.

nanoparticles the strong hydrogen bonding between the surface and the coating agent reflects a decrease in the positive zeta potential and the small size favours the penetration into the cancer cell line thereby inhibiting its growth.[22] Thus, the size and the surface charge distribution of functionalized nanoparticles anticipated the anti-cancer activity.

3.4 *Magnetic properties*

At the atomic level, the magnetic properties originate from the quantum coupling including coupling between electron spin (S-S coupling) and the coupling between the electron spin and angular momentum of the electron orbital (L-S coupling).[25] Paramagnetic materials have a tendency to align with the magnetic dipole with an external magnetic field due to their small positive susceptibility and their random orientation in the absence of magnetic field. Superparamagnetic materials have much larger susceptibility as the entire crystals aligns with the applied field.[26] Figure 6 shows the relative magnetization curves of the bare and coated magnetite nanoparticles as a function of magnetic field. The samples exhibited superparamagnetic behaviour due to the symmetric hysteresis and saturation magnetization which means that they are attracted by external magnetic field but retain no residual magnetism when the external magnetic field is removed at room temperature. Table 1 shows coercivity and magnetization values of bare and coated magnetite nanoparticles. The coercivity

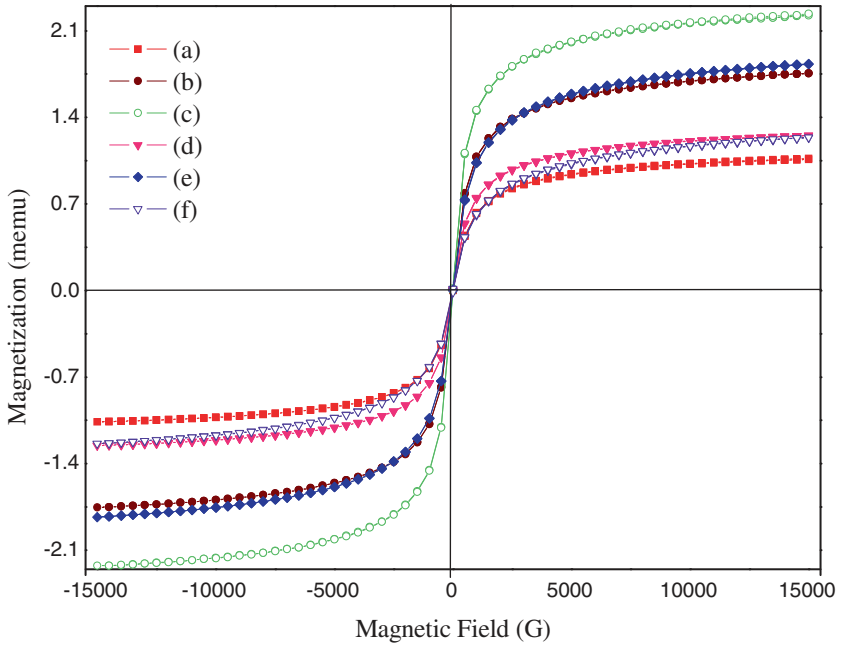

Figure 6. Magnetization curves of (**a**) Fe_3O_4 nanoparticles; and nanoparticles coated with (**b**) Ascorbic acid; (**c**) Hexanoic acid; (**d**) Salicylic acid; (**e**) L-Arginine; (**f**) L-Cysteine.

Table 1. Coercivity and magnetization values for the synthesized nanoparticles.

Samples	Coercivity HC_i Gauss	Magnetization Ms (memu/mg)
S	1.5712	1.0645
S1	3.5794	1.7552
S2	5.1393	2.2312
S3	0.9190	1.8323
S4	1.8260	1.8323
S5	16.334	1.2387

and the remanence values are not discernible indicating a superparamagnetic behaviour. The Ms value of bare iron oxide nanoparticles is 1.0 memu/mg and that of acid coated iron oxide nanoparticles ranges between 1.2387 and 2.2312 memu/mg. The lower magnetization value of bare magnetite when compared to the coated materials is due to easy transformation of magnetite to other phases with temperature.[2] This difference in Ms value of the magnetic behaviour is mainly due to the decrease in particle size due to the reduction in crystallinity. The best way to increase the Ms value is to increase the crystalline size.

The high saturation magnetization of hexanoic acid coated nanoparticles indicated its good crystal structure. The changes of Ms value are correlated with the change of magnetic particle size and also the purity of the magnetite.[27] Magnetization of the samples increases with external magnetic field which is the characteristic feature of superparamagnetic behaviour. This difference may give rise to non-collinear spin arrangement near the surface occurring due to the reduction of magnetic moment in iron oxide nanoparticles.[28] Thus, such

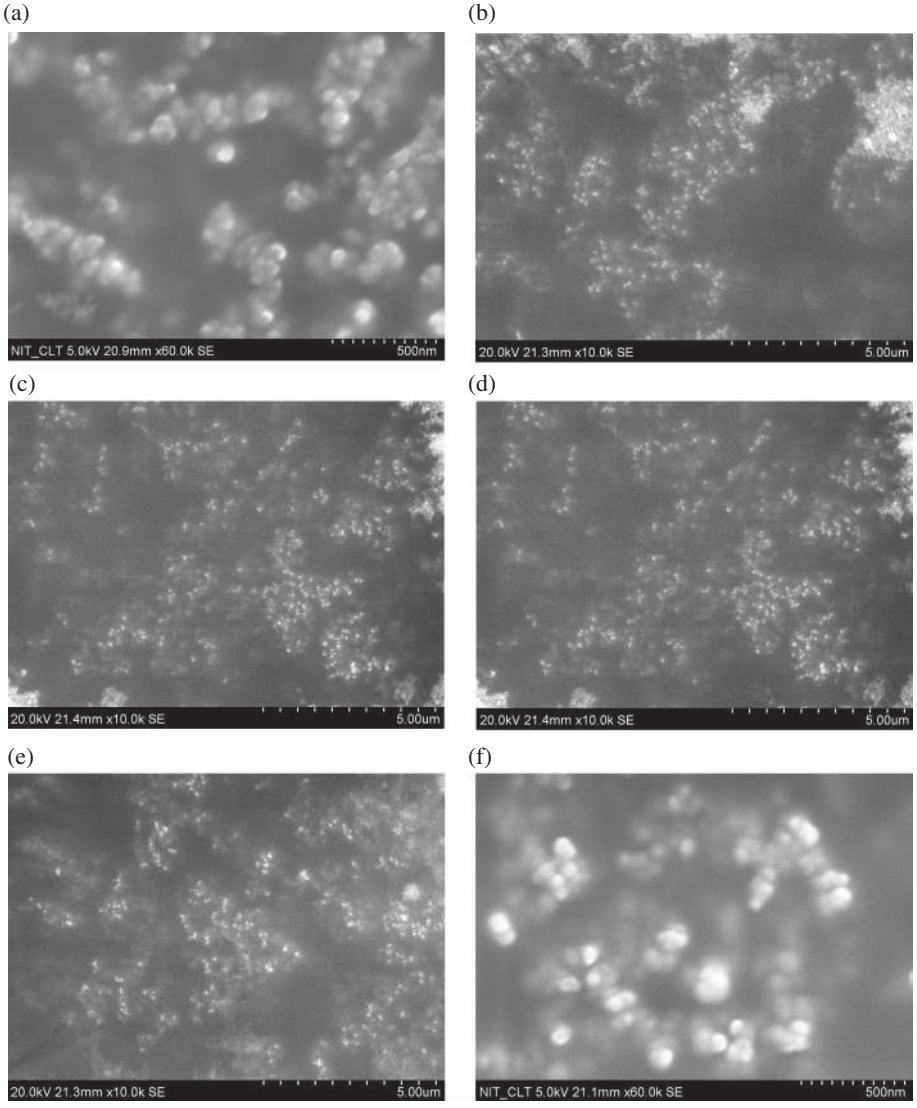

Figure 7. SEM images of (**a**) Fe_3O_4 nanoparticles; and nanoparticles coated with (**b**) Ascorbic acid; (**c**) Hexanoic acid; (**d**) Salicylic acid; (**e**) L-Arginine; (**f**) L-Cysteine.

nanoparticles can be used as magnetic carriers which have good potential and broad application in drug delivery and hence can be used for the treatment of cancer in near future.

3.5 *SEM and TEM analysis*

FESEM micrographs (figure 7) display the morphology of the Fe_3O_4 nanoparticles. The shape of Fe_3O_4 nanoparticles is roughly spherical and with rough particle surface which will be useful for further surface coatings. The presence of rough surface suggests that these particles grow by aggregation of the small particles. The growth of large particles at the expense of smaller ones so as to achieve a minimum of total free energy by the tendency of solid phase in the system is described as Ostwald ripening.[29] The images also indicate that these particles show good dispersion resulting from the protection of coatings on the surface of nanoparticles.

Transmission electron microscopy (TEM) images of L-arginine coated nanoparticles with different magnification shows that all the particles are spherical in shape (figure 8). TEM images revealed that the particle size for bare iron oxide nanoparticle is 31 nm and that of L-arginine coated nanoparticles was 26 nm. This decrease in size is may be due to the coating agent, which prevents agglomeration and hence reduces the size of the nanoparticles. The nucleation rate per unit area is isotopic at the interphase between the iron oxide nanoparticles and hence gives rise to spherical shape.[30] However, small particles have larger surface area-to-volume ratio and represent a higher energy state than large particles. The crystallization of L-arginine coated magnetite nanoparticles showed no reduction in magnetic property and the growth was prevented because of the steric hindrance of coating agent.

3.6 *TGA-DSC analysis*

The results of TGA-DSC show that the initial weight loss at a temperature below 120°C refers to the evaporation of adsorbed water (figure 9). The slight increase in weight above 500°C corresponds to the transformation of the magnetite to hematite.[31]

Thermogram of the coated nanoparticles indicates three step weight loss, first step is due to desorption of water molecule at temperature below 120°C. The second weight loss at 310°C and the third at 450°C is due to the decomposition of the physisorption and the chemisorptions of the coating agent at the surface of magnetite nanoparticles, respectively.[32] The corresponding DSC curve of L-arginine and hexanoic acid coated nanoparticles exhibit an endothermic peak between 250°C and 270°C due to the oxidation and change in crystallinity of Fe_3O_4. Decomposition of L-arginine coated nanoparticles occurs at about 617°C producing an exothermic peak whereas hexanoic acid coated nanoparticles exhibited peak at 580°C proving that L-arginine coated nanoparticles is more stable and oxidized at higher temperature than hexanoic acid coated nanoparticles.[33]

3.7 *In vitro cytotoxicity*

The anti-cancer activity of bare, acid coated and paclitaxel drug loaded L-arginine coated nanoparticles on human lung cancer A549 cell line was determined using MTT assay (figure 10). The assay measures the cell proliferation rate leading to apoptosis and reduces the cell viability. This is a colorimetric assay that measures the reduction of yellow MTT by mitochondrial succinate dehydrogenase. The MTT enters the cells and passes into the mitochondria where it is reduced to an insoluble, coloured (dark purple) formazan product. Percentage cell viability was determined using different concentration

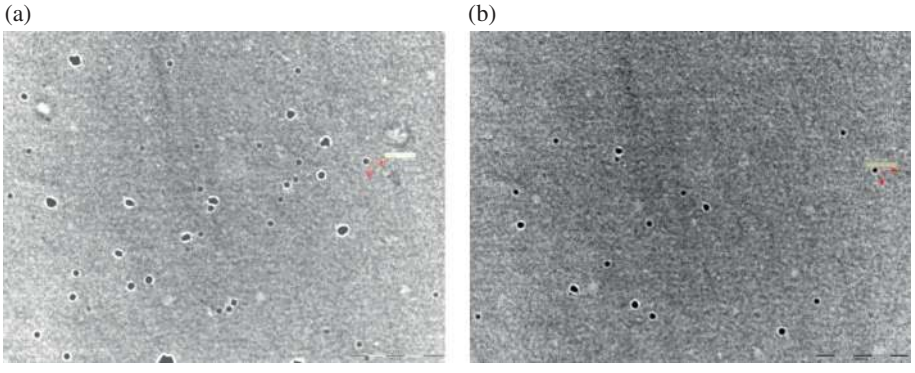

Figure 8. TEM images of (**a**) Fe_3O_4 nanoparticles; and (**b**) L-Arginine coated Fe_3O_4 nanoparticles.

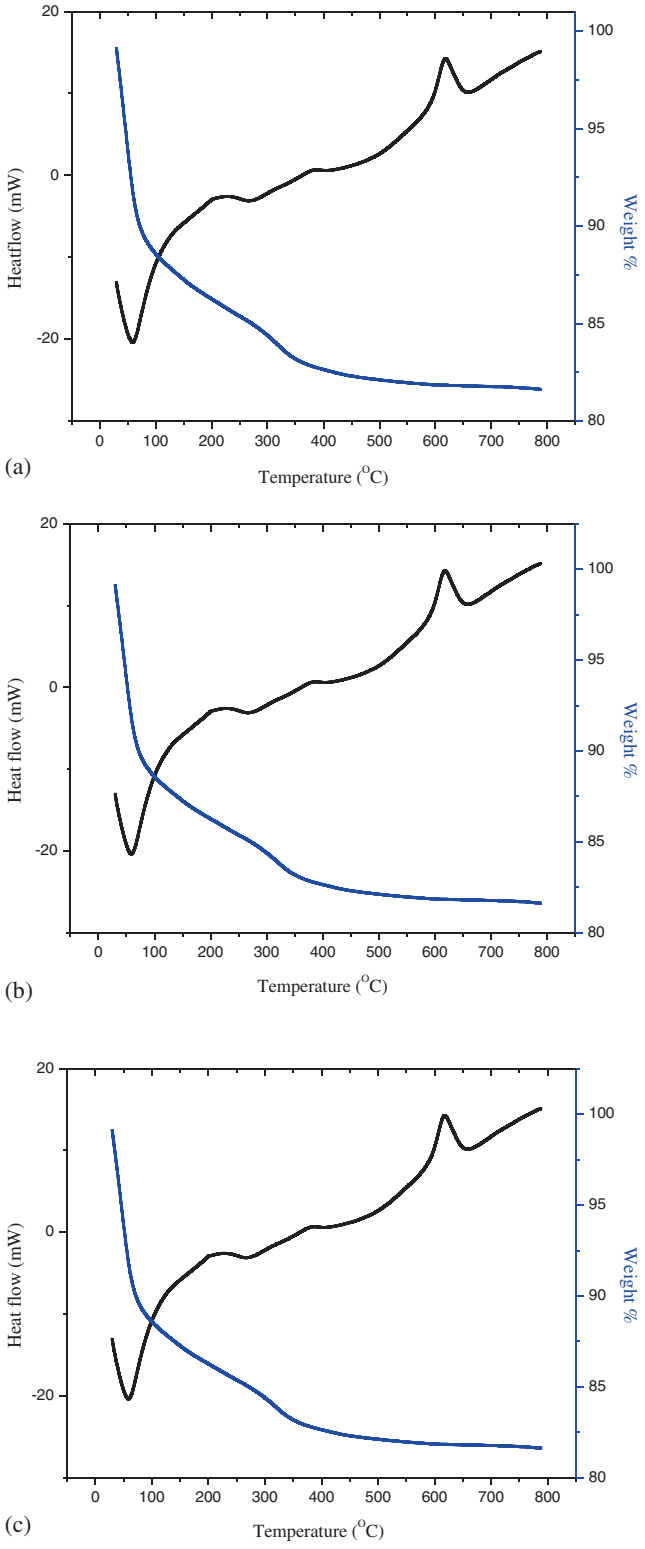

Figure 9. TGA-DSC analysis of (**a**) Fe_3O_4 nanoparticles; and nanoparticles coated with (**b**) Hexanoic acid; (**c**) L-Arginine.

of the bare and coated nanoparticles and the compatability of nanocarriers was determined graphically by IC_{50} values at an absorbance of 540 nm (table 2).

The IC_{50} value of bare and L-arginine coated iron oxide nanoparticles was found to be 31.2 μg/mL, whereas that of ascorbic acid, hexanoic acid, salicylic acid and L-cysteine coated nanoparticles was 62.5 μg/mL. The drug alone had IC_{50} value of 15.6 μg/mL whereas paclitaxel drug loaded L-arginine coated nanoparticles exhibited an IC_{50} value of 7.8 μg/mL (figure 11). The paclitaxel drug loaded on L-arginine coated nanoparticles were found to be more effective in inhibiting the growth of cancer cells when compared to the native paclitaxel. The magnetic force acting on the magnetic particle is proportional to the volume of the particle as the material is superparamagnetic. The magnetic force experienced by the smaller particles overcomes the force by the fluidic drag. Therefore, small particles have good permeability but poor retention. The anti-cancer drug paclitaxel has affinity to the targe t cells and after grafting the drug to the surface magnetic nanoparticles can be internalized more rapidly.[34]

L-Arginine coated iron oxide nanoparticles produced significant cytotoxicity when compared to the other coated nanoparticles and resembled the bare iron oxide nanoparticles. The similarity in cytotoxicity of the bare and L-arginine functionalized magnetite nanoparticles may be due to the same particle size as already been reported.[35] The anti-cancer activity of L-arginine coated iron oxide nanoparticles on non-cancer cell line (vero cell line) was studied. L-Arginine coated nanoparticles exhibited 80% of cell viability at a concentration of 31.2% μg/mL proving that it can be utilized as a promising platform for biomedical application (table 3).

L-Arginine coated nanoparticles with incubation at higher concentration caused significant cell death (80%). However, it is expected that such a higher concentration of 1000 μg/mL will not be used for *in vivo* applications. Preliminary studies have proved that 15 μg/mL of L-arginine was enough to cause cell death. Due to cytotoxic nature of paclitaxel treatment with drug loaded nanopartciles showed a decrease in cell viability of 51.2±0.1 at 7.8 μg/mL concentration.[5]

3.8 *DNA fragmentation*

DNA fragmentation is a key feature of apoptosis, a type of programmed cell death. DNA is degraded into smaller fragments of oligonucleosomal size and is visualized as a laddering pattern in an agrose gel electrophoresis.[36] Systematic cleavage of DNA to produce nucleosomal fragments of 200 bp (or its multiples) is considered as characteristic of apoptosis.[37]

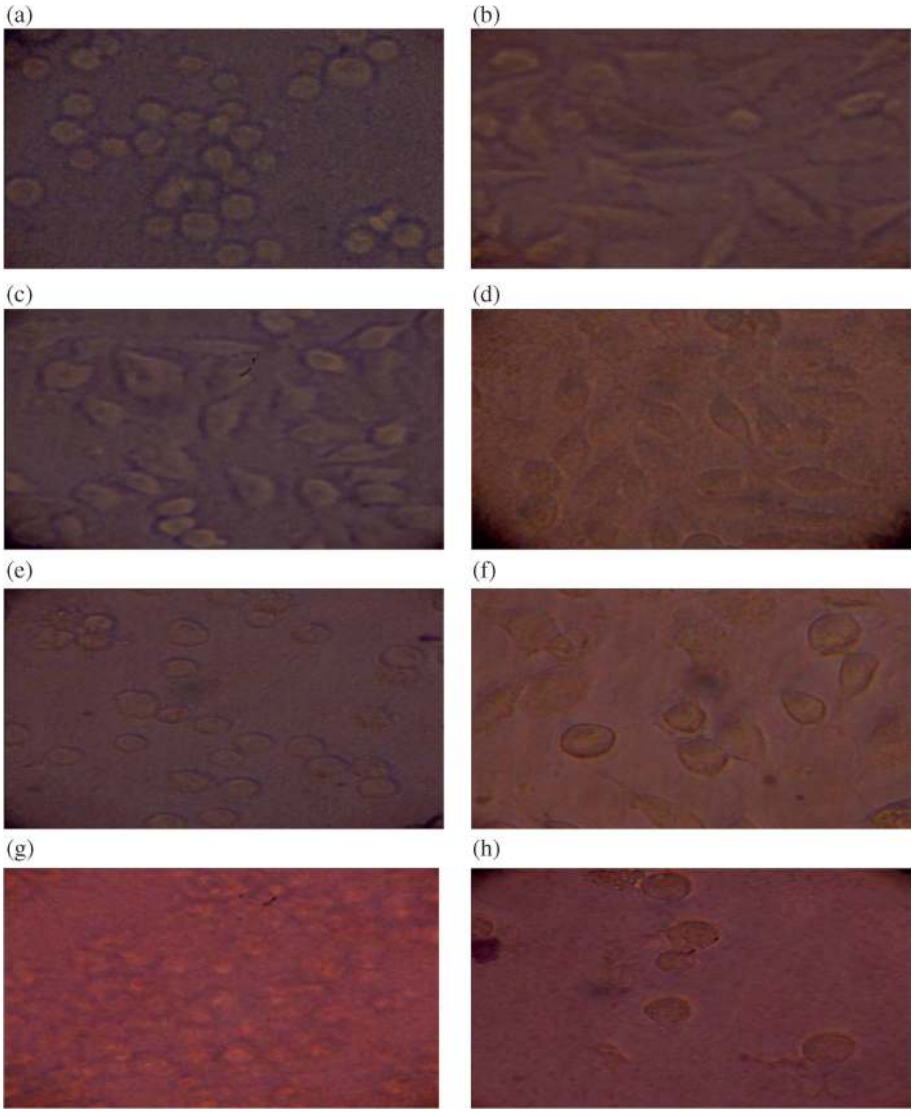

Figure 10. The morphological changes of human lung cancer cell line (A549) by MTT assay. (**a**) Fe_3O_4 nanoparticles; and nanoparticles coated with (**b**) Ascorbic acid; (**c**) Hexanoic acid; (**d**) Salicylic acid; (**e**) L-Arginine; (**f**) L-Cysteine; (**g**) Drug paclitaxel alone; and (**h**) Drug paclitaxel loaded L-arginine coated nanoparticles.

Table 2. IC_{50} values of bare and coated nanoparticles.

Samples	IC_{50} values	Cell viability
S	31.2	49.2±0.20
S1	62.5	46.5±0.15
S2	62.5	46.5±0.15
S3	62.5	54.1±0.1
S4	31.2	53.5±0.15
S5	62.5	52.3±0.2
S6	15.6	53.5±0.15
S7	7.8	51.2±0.1

The IC_{50} value of L-arginine coated nanoparticles (31.2 μg/mL) proving its effectiveness in inhibiting A549 cell growth when compared with other coated nanoparticles. To elucidate whether the L-arginine coated nanoparticles inhibit proliferation through induction of apoptosis, DNA fragmentation was observed by agrose gel electrophoresis (figure 12). The breakdown of DNA molecules at a concentration of 1 mg/mL proved the inhibition of DNA replication, while untreated cells did not show any DNA fragmentation. Cell studies revealed that L-arginine functionalized nanoparticles was far more effective in inhibiting tumour proliferation by inducing apoptosis as indicted by the presence

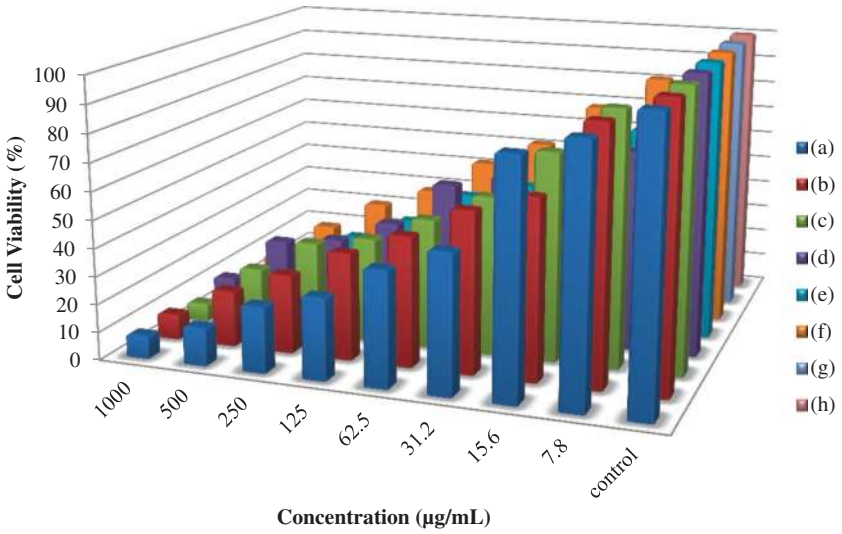

Figure 11. Percentage cell viability of nanoparticles at different concentration using MTT assay. (**a**) Fe_3O_4 nanoparticles; and nanoparticles coated with (**b**) Ascorbic acid; (**c**) Hexanoic acid; (**d**) Salicylic acid; (**e**) L-Arginine; (f) L-Cysteine. (**g**) Drug paclitaxel alone; and (**h**) Drug paclitaxel loaded L-arginine Fe_3O_4 coated nanoparticles.

Table 3. Percentage cell viability at different concentration of L-arginine coated nanoparticles for normal cell lines.

Sl. No.	Concentration μg/mL	Dilution	Absorbance 540 nm	% Cell viability
1	1000	Neat	0.21	19.0
2	500	1:1	0.43	39.0
3	250	1:2	0.58	52.7
4	125	1:4	0.79	71.8
5	62.5	1:8	0.85	77.2
6	31.2	1:16	0.88	80.0
7	15.6	1:32	0.93	84.5
8	7.8	1:64	1.03	93.6
9	control	-	1.10	100

of DNA fragmentation in treated cancer cells. Thus, the present study supports the anti-proliferative activity of L-arginine functionalized nanoparticles against A549 human lung cancer cell lines.

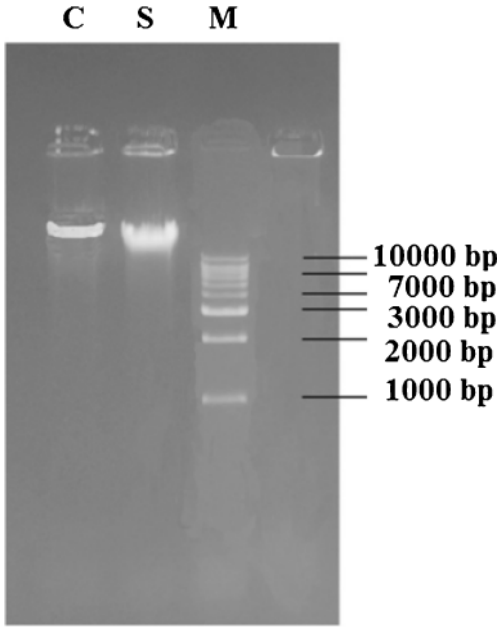

Figure 12. DNA fragmentation of A549 cells treated with L-arginine coated magnetite nanoparticles. The image shows untreated cells (**C**); cell treated with L-arginine coated Fe_3O_4 nanoparticles (**S**) and the marker (**M**). The untreated cells showed no evidence of fragmentation.

4. Conclusions

Superparamagnetic, bare and acid functionalized magnetite nanoparticles with efficient biocompatibility have been synthesized by co-precipitation method. XRD analysis suggested cubic spinal structure of the nanoparticles. Zeta measurements of L-arginine coated nanoparticles exhibited a lower potential and increase in the particle size due to the obstruction of intermolecular hydrogen bonding and positive charge of the amino group. The samples showed superparamagnetic behaviour with symmetric hysteresis and saturation magnetization. The TEM images revealed the crystalline size to be 31 nm for the bare iron oxide nanoparticles and 26 nm for L-arginine coated iron

oxide nanoparticles. Further, all the synthesized magnetite nanoparticles were tested for biomedical application as magnetic carriers. Cytotoxicity tests on A549 cell lines using MTT assay to find out % cell viability for various concentrations were performed. Paclitaxel drug loaded with L-arginine nanoparticles resulted in enhanced cytotoxic effect leading to apoptosis. DNA fragmentation on A549 cell line with L-arginine coated iron oxide nanoparticles and control cells were examined. The control cells did not show any proliferation, whereas L-arginine coated iron oxide nanoparticles showed DNA fragmentation, proving that amino acid functionalized magnetite nanoparticles provided new opportunities for application in anti-cancer treatment.

Acknowledgement

DR thanks UGC, SERO, Hyderabad, for the financial support through the Minor Research Project Grant (No. F./MRP- 3984/11).

References

1. Tran N and Webster T J 2010 *J. Mater. Chem.* **20** 8760
2. Petcharoen K and Sirivat A 2012 *Mater. Sci. Eng. B* **177** 421
3. Mohapatra M and Anand S 2010 *Int. J. Eng. Sci. Technol.* **2** 127
4. Ozkaya T, Toprak M S, Baykal A, Kavas H, Koseoglu Y and Aktas B 2009 *J. Alloys Compd.* **472** 18
5. Rastogi R, Gulati N, Kotnala R K, Sharma U, Jayasundar R and Koul V 2011 *Colloids Surf. B: Biointerfaces* **82** 160
6. Gupta A K and Gupta M 2005 *Biomaterials* **26** 1565
7. Tan W L and Abubakar M 2006 *J. Phys. Sci.* **17** 37
8. Narain R, Gonzales M, Hoffmann A S, Stayton P S and Krishnan K M 2007 *Langmuir* **23** 6299
9. Tomitaka A, Hirukawa A, Yamada T, Morishita S and Takemura Y 2009 *J. Magn. Magn. Mater.* **321** 1482
10. de Sousa M, van Raap M B F, Rivas P C, Zéils P M, Girardin P, Pasquevich G A, Alessandrini J L, Muraca D and Sánchez F H 2013 *J. Phys. Chem. C* **117** 5436
11. Suri S S, Fenniri H and Singh B 2007 *J. Occup. Med. Toxicol.* **2** 1
12. Andhariya N, Chudasama B, Mehta R V and Upadhyay R V 2011 *J. Nanopart. Res.* **13** 1677
13. Lee K J, An J H, Shin J S, Kim D H, Yoo H S and Cho C K 2011 *Curr. Appl. Phys.* **11** 467
14. Bakshi H, Sam S, Rozati R, Sultan P, Islam T, Rathore B, Lone Z, Sharma M, Triphati J and Saxena R C 2010 *Asian Pac. J. Cancer. Prev.* **11** 675
15. Zheng Y Y, Wang X B, Shang L, Li C R, Cui C, Dong W J, Tang W H and Chen B Y 2010 *Mater. Charact.* **61** 489
16. Kim D K, Zhang Y, Voit W, Rao K V and Muhammed M 2001 *J. Magn. Magn. Mater.* **225** 30
17. Lui X, Kaminski M D, Guan Y, Chen H, Lui H and Rosengart A J 2006 *J. Magn. Magn. Mater.* **306** 248
18. Chen C, Jiang X, Kaneti Y V and Yu A 2013 *Powder Technol.* **236** 157
19. Ghavami M, Koohi M and Kassae M Z 2013 *J. Chem. Sci.* **6** 1347
20. Feng L, Cao M, Ma X, Zhu Y and Hu C 2012 *J. Hazard. Mater.* **217** 439
21. Karaoglu E, Baykal A, Senel M, Sozeri H and Toprak M S 2012 *Mater. Res. Bull.* **47** 2480
22. Bhattacharya D, Sahu S K, Banerjee I, Das M, Mishra D, Maiti T K and Pramanik P 2011 *J. Nanopart. Res.* **9** 4173
23. Giri J, Thakurta S G, Bellare J, Nigam A K and Bahadur D 2005 *J. Magn. Magn. Mater.* **293** 62
24. Karaagac O, Kockar H, Beyaz S and Tarisever T 2010 *IEEE Trans. Magn.* **46** 3978
25. Sharifi I, Shokrollahi H, Doroodmand M M and Safi R 2012 *J. Magn. Magn. Mater.* **324** 1854
26. Thorek D L J, Chen A K, Czupryna J and Tsourkas A 2006 *Ann. Biomed. Eng.* **34** 23
27. Daou T J, Greneche J M, Pourroy G, Buathong S, Derory A, Ulhaq-Bouillet C, Donnio B, Guillon D and Begin-Colin S 2008 *Chem. Mater.* **20** 5869
28. Wei Y, Han B, Hu X, Lin Y, Wang X and Deng X 2012 *Procedia. Eng.* **27** 632
29. Ni S, He D, Yang X and Li T 2011 *J. Alloys. Compd.* **509** L305
30. Lu W, Shen Y, Xie A and Zhang W 2010 *J. Magn. Magn. Mater.* **322** 1828
31. Yuana P, Fana M, Yanga D, He H, Liu D, Yuan A, Zhu J X and Chen T H 2009 *J. Hazard. Mater.* **166** 821
32. Grumezescu A M, Gestal M C, Holban A M, Grumezescu V, Vasile B S, Mogoanta L, Iordache F, Bleotu C and Mogosanu G D 2014 *Molecules* **19** 5013
33. Huang C, Zhang H, Sun Z, Zhao Y, Chen S, Tao R and Liu Z 2011 *J. Colloid Interface Sci.* **364** 298
34. Kayal S and Ramanujan R V 2010 *J. Nanosci. Nanotechnol.* **10** 1
35. Ebrahiminezhad A, Ghasemi Y, Rasoul-Amini S, Barar J and Davaran S 2012 *Bull. Korean Chem. Soc.* **33** 3957
36. Guimarais V I, Guinon E G, Gabernet G, Gareia-Belinchon G, Sanchez-Osuna M, Casanelles E, Comella J X and Yuste V J 2012 *J. Biol. Chem.* **287** 7766
37. Talib W H, Issa R A, Kherissat F and Mahasneh A M 2013 *Br. J. Med. Med. Res.* **3** 771